Available online at www.sciencedirect.com
ScienceDirect
Engineering Fracture Mechanics 75 (2008) 1794–1803
Engineering Fracture Mechanics
www.elsevier.com/locate/engfracmech

Atomistic fracture: QFM vs. MD ☆

Nicola Pugno [a,*], Alberto Carpinteri [a], Mariella Ippolito [b], Alessandro Mattoni [b], Luciano Colombo [b]

[a] *Department of Structural Engineering and Geotechnics, Politecnico di Torino, Torino, Italy*
[b] *INFM-SLACS and Department of Physics, University of Cagliari, Cagliari, Italy*

Received 25 October 2006; received in revised form 29 January 2007; accepted 31 January 2007
Available online 16 February 2007

Abstract

In this work we discuss the paradigmatic case of brittle fracture in defective elastic–plastic cubic silicon carbide, by a combination of Quantized Fracture Mechanics and Molecular Dynamics atomistic simulations. Different defect sizes and shapes, or crack-inclusion interactions are considered. Our results show that Quantized Fracture Mechanics is able to effectively incorporate the main lattice-related features, while Molecular Dynamics atomistic simulations do provide the most basic level of understanding of mechanical behaviour of brittle materials.

Keywords: Atomistic; Fracture; QFM; MD

1. Introduction

Traditional analysis of brittle fracture resorts to the well established Griffith's theory [1], which describes the crack growth by the related energy balance. The result is that a crack of given length propagates at the critical value of the applied load for which the variation (with respect to the crack surface) of the total potential energy (elastic energy minus external work) of the system reaches a critical material characteristic G_c. In a perfect elastic solid in vacuum the crack resistance energy per unit surface is identified with the (unrelaxed) cleavage surface energy 2γ [2,3]. The Griffith's criterion [1] was extensively verified in glass specimens containing cracks of controlled length and it is still adopted to estimate the surface energy of brittle materials [2,4]. Formally, G_c is defined as $G_c = 2\gamma_c$ where the material parameter γ_c is the integral of the stress vs. separation curve for the atomic planes undergoing separation during the fracture process. The factor of 2 accounts for the creation of two surfaces during crack formation. While within Linear Elastic Fracture Mechanics (LEFM) it is

☆ This article appeared in its original form in *Fracture of Nano and Engineering Structures: Proceedings of the 16th European Conference of Fracture, Alexandroupolis, Greece, July 3–7, 2006* (Edited by E.E. Gdoutos, 2006). Springer, Dordrecht, The Netherlands. ISBN 1-4020-4971-4.

* Corresponding author.
E-mail address: nicola.pugno@polito.it (N. Pugno).

0013-7944/$ - see front matter
doi:10.1016/j.engfracmech.2007.01.028

typically assumed that $\gamma_c = \gamma$, γ_c includes in general also other atomic level details and other form of dissipations such as plasticity [5–8].

Recently, a new energy-based theory, namely Quantized Fracture Mechanics (QFM [9,10]), that modifies continuum-based fracture mechanics substituting the differentials in Griffith's energy balance with finite differences, has been formulated. This simple assumption has remarkable implications: QFM can be applied to defects of any size and shape, in contrast to LEFM that can treat only "large" and perfectly sharp cracks. Such an approach has been very recently extended to derive an even more general theory, namely, Dynamic Quantized Fracture Mechanics (DQFM [11]), applicable also to dynamic fracture, e.g., impacts, where classical Dynamic Fracture Mechanics reveals limitations. Extensions in different fields, such as fatigue crack growth, have been also proposed [12]. Applications of previous concepts have been reported in a series of different papers [13–15].

Furthermore, Molecular Dynamics (MD) atomistic simulations offer the opportunity to study the fundamental issues underlying the Griffith's theory in ideally pure, perfect single-crystal materials. In this work we present an atomic-scale numerical investigation of brittle fracture computing the strength of defective crystals considering different types of voids or inclusions. In particular for cracks, we find that the identification of crack resistance γ_c with the cleavage surface energy γ provides only a lower limit to the energy release rate. As a matter of fact, γ_c is not a constant (i.e., we found the atomistic equivalent of the classical R-curve macroscopic behaviour), depending both on the crack length and on the deformation state [16].

We have also considered the influence on the stress-intensity factor at the crack tip due to the interaction between the crack and an hard (carbon) or soft (silicon) inclusion in the silicon carbide matrix [17] and different types of defects, such as spherical or elliptical voids [18]. We have focused our work on cubic silicon carbide (β-SiC) since it is the prototype of an ideally brittle material up to extreme values of strain, strain rate and temperature, and because of its technological relevance as a structural and nuclear material. The available data for β-SiC are accurate enough (despite the microstructural heterogeneities of experimental samples) to suggest that its intrinsic crack resistance in vacuum is, indeed, higher than the theoretical, ideal-crystal surface energy.

QFM, in agreement with the MD findings, shows deviations from classical strength predictions (based on stress-intensifications or -concentrations in a continuum), mainly imposed by the lattice discreteness.

2. Atomistic cracks and holes

The QFM theory [9,10] introduces a quantization of the Griffith's criterion to account for discrete crack propagation, and thus in the continuum hypothesis differential are substituted with finite differences, i.e., $d \to \Delta$ [9]. According to the principle of conservation of energy, Griffith's criterion implies a crack propagation when the variation of the total potential energy dW, corresponding to a virtual increment of the crack surface dA, becomes equal to the energy spent to create the new free crack surface, i.e., $dW + G_c dA = 0$. The energy release rate is defined as $G = -dW/dA$ (where the derivation is evaluated at constant displacement) and Griffith's criterion is simply $G = G_c$. For finite differences it becomes $G^* = -\Delta W/\Delta A = G_c$. QFM assumes dissipation energy in discrete amounts $G_c \Delta A$, where ΔA is the minimum crack surface increment. The hypothesis on which QFM is based is discrete crack propagation in a (linear elastic, but we are going to relax this hypothesis) continuum medium. LEFM is so modified to account for the material heterogeneities (e.g., grains) or, in our context, for the intrinsic discontinuous nature of matter at the atomic scale, see Fig. 1. If the applied load is not quasi-static, DQFM would have to be considered in stead of QFM.

Consider the Griffith's case of a linear elastic infinite plate in tension, of uniform thickness, with a crack of length $2c$ orthogonal to the applied far field (crack opening Mode I, Fig. 2a). According to QFM and adopting as minimum crack advancement the interbond distance along the plane of the crack c_0 (Fig. 1) the failure stress for a crack with small tip radius r is [10]

$$\sigma_C^{QFM}(c,r) = \sqrt{\frac{2\gamma_C(c,r)E'}{\pi c}}, \quad \gamma_C(c,r) = \gamma \frac{1 + r/2c_0}{1 + (c_0/2c)}; \quad \text{or} \quad \frac{\sigma_C^{QFM}(c,r)}{\sigma_{th}} = \sqrt{\frac{1 + r/2c_0}{1 + (2c/c_0)}} \tag{1}$$

whereas according to Griffith $\gamma_c \equiv \gamma$ is a constant. In the above expression $E' = E$ for plane stress, and $E' = E/(1 - \nu^2)$ for plane strain, where E and ν are the Young's modulus and Poisson' ratio respectively of the considered material. Note that, in contrast to LEFM, QFM can predict the ratio between failure stress and theoretical (defect-free) σ_{th} strength.

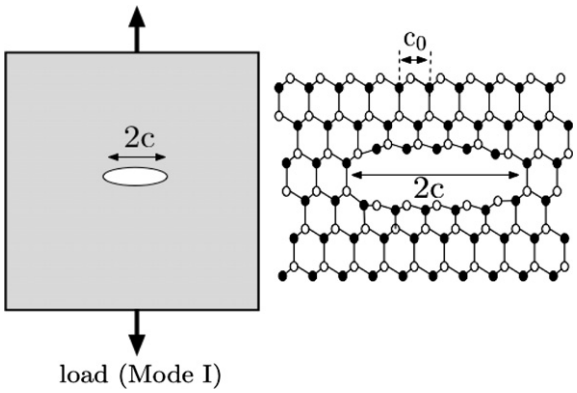

Fig. 1. Left: geometry of the Griffith's plate, for Mode I loading (LEFM). Right: the corresponding atomic-scale picture (QFM).

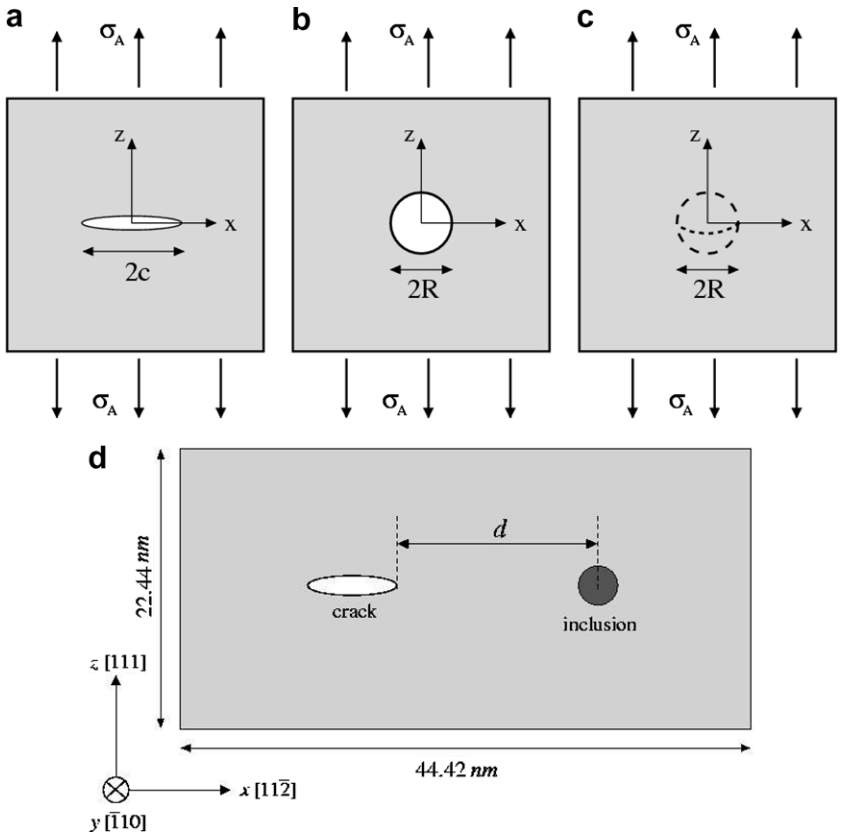

Fig. 2. Investigated schemes: (a) cracks, (b) cylindrical or (c) spherical holes and (d) crack-inclusion interaction.

We can also treat spherical or cylindrical [10] holes (Fig. 2b and c). For them the stress-intensity factor (of a small crack emanated from the hole) is numerically known (from the stress-intensity factor handbooks). The QFM strength predictions [10] are in agreement with those derived according to the Novozhilov's approach [19], that is the stress analog of QFM. Thus, for a cylindrical hole of radius R we have deduced [10]

$$\frac{\sigma_C^{QFM}(R)}{\sigma_{th}} = \frac{2}{2 - \frac{R}{c_0}\left(\frac{1}{1+c_0/R} - 1\right) - \frac{R}{c_0}\left(\frac{1}{(1+c_0/R)^3} - 1\right)} \tag{2}$$

whereas for a spherical hole [18]

$$\frac{\sigma_C^{\mathrm{QFM}}(R)}{\sigma_{\mathrm{th}}} = \frac{2}{2 - \frac{4-5\nu}{2(7-5\nu)}\frac{R}{c_0}\left(\frac{1}{(1+c_0/R)^2}-1\right) - \frac{9}{4(7-5\nu)}\frac{R}{c_0}\left(\frac{1}{(1+c_0/R)^4}-1\right)} \tag{3}$$

3. Elastic–plastic or hyper-elastic materials and fractal cracks

The previous equations are based on linear elasticity, i.e., on a linear relationship $\sigma \propto \varepsilon$ between stress σ and strain ε. In contrast, let us assume $\sigma \propto \varepsilon^{\kappa}$, where $\kappa > 1$ denotes hyper-elasticity, as well as $\kappa < 1$ elastic–plasticity. The power of the stress-singularity will accordingly be modified [20] from the classical value 1/2 to $\alpha = \kappa/(\kappa+1)$. Thus, the problem is mathematically equivalent to that of a re-entrant corner, and consequently from its solution [21] we predict

$$\frac{\sigma_C^{\mathrm{QFM}}(\alpha)}{\sigma_{\mathrm{th}}} = \left(\frac{\sigma_C^{\mathrm{QFM}}(\alpha = 1/2)}{\sigma_{\mathrm{th}}}\right)^{2\alpha}, \quad \alpha = \frac{\kappa}{\kappa+1} \tag{4}$$

A crack with a self-similar roughness, mathematically described by a fractal with non-integer dimension $1 < D < 2$, would similarly modify the stress-singularity, according to $\alpha = (2-D)/2$ [22,23]; thus, with Eq. (4), we can also estimate the role of the crack self-similar roughness. Both plasticity and roughness reduce the severity of the defect, whereas hyper-elasticity enlarges its effect. For example, for a sharp crack composed by $n = 2c/c_0$ adjacent vacancies, we found from Eq. (1) $\sigma_C^{\mathrm{QFM}}/\sigma_{\mathrm{th}} \approx (1+n)^{-\alpha}$. Note that, in the limit of small cracks, the treated nonlinearities fictitiously modify c_0: for the previous example we find $c_0 \to c_0/(2\alpha)$. Similar results hold also for different kinds of defects, such as cylindrical or spherical holes. Thus, different c_0 are expected for the same lattice treating problems with different nonlinearities.

For a fractal crack, writing the corresponding energy balance, we predict the propagation for $K = K_C^{(D)}$, where K is the stress-intensity factor at the crack tip and $K_C^{(D)} \equiv \sqrt{2DE'\gamma_C^{(D)}C^{D-1}}$ is the equivalent fracture toughness of the fractal crack [22,23]; $\gamma_C^{(D)}$ is thus the fractal fracture energy and $K_C^{(1)} = K_C$ is the classical material fracture toughness. Since according to QFM [10–12] $K^{(c_0)} \equiv \sqrt{\langle K^2\rangle_c^{c+c_0}} = K_C$ ($\langle\rangle$ denotes the mean value operator), for a fractal crack the propogation will take place for $K^{(c_0)} = K_C^{(c_0,D)} \equiv \sqrt{\langle K_C^{(D)2}\rangle_c^{c+c_0}} = \sqrt{2E'\gamma_C^{(D)}[(c+c_0)^D - c^D]/c_0}$ or, equivalently, for $K^{(c_0,D)} \equiv \frac{K^{(c_0)}K_C}{K_C^{(c_0,D)}} = K_C$. This fracture propagation criterion represents a Quantized Fractal Fracture Mechanics and the derived definitions of $K_C^{(c_0,D)}$ and $K^{(c_0,D)}$ can be used to

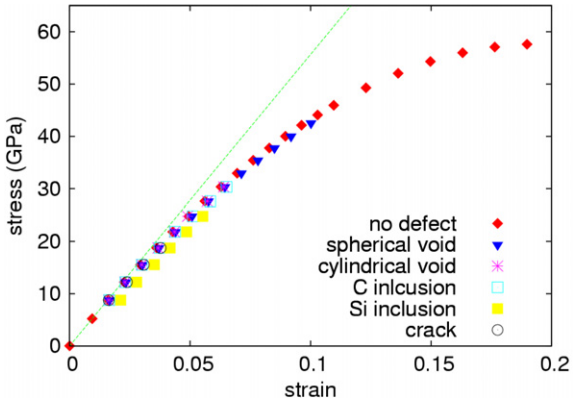

Fig. 3. Example of stress–strain curves computed by atomistic simulations. Note the elastic–plastic constitutive law of the defect-free crystal, as well as the effect on strength and elasticity of the investigated defects (crack length of 3.6 nm, voids and isolated inclusions of 1 nm in diameter).

generalize in a fractal sense all the quantized failure criteria (e.g., also in dynamic fracture and fatigue) proposed by the first author [12].

An elastic–plastic behaviour has been atomistically computed for the investigated β-SiC crystal, see Fig. 3. Fitting the atomistic stress–strain curve for the investigated defect-free β-SiC crystal, we find $\kappa \approx 0.81$ and thus $\alpha \approx 0.45$. Accordingly, the correction reported in this section is expected to play a role, especially for the failures at higher strain levels, thus for holes, whereas for cracks, failures basically take place in the linear elastic region (see Fig. 3).

4. Interaction crack-inclusion

Now let us consider a small inclusion collinear with the crack at distance d from its tip (Fig. 2d). According to the Eshelby's classical solution the variation of the stress-intensity factor due to the presence of the inclusion is $\Delta K_{\mathrm{tip}}/K = c_1/d^2$ (see [24]). On the other hand, assuming a discrete crack advancement the following deviation is expected [17]:

$$\frac{\Delta K_{\mathrm{tip}}^{\mathrm{QFM}}}{K} = \frac{c_1}{d^2}\sqrt{\frac{1 + c_0/d + 1/3(c_0/d)^2}{(1 + c_0/d)^3}} \approx \frac{c_1}{d^2(1 + c_0/d)} \tag{5}$$

Note that the last approximated equality is valid in the limit of $c_0/d \to 0$ and it is identical to that predicted according to the Novozhilov's approach [19].

5. Atomistic MD simulations and QFM comparison

We have carried out damped MD atomistic simulations with the aim of reproducing the macroscopic conditions of a quasi-static (or adiabatic) crack loading process at 0 K. Atomic forces were calculated according

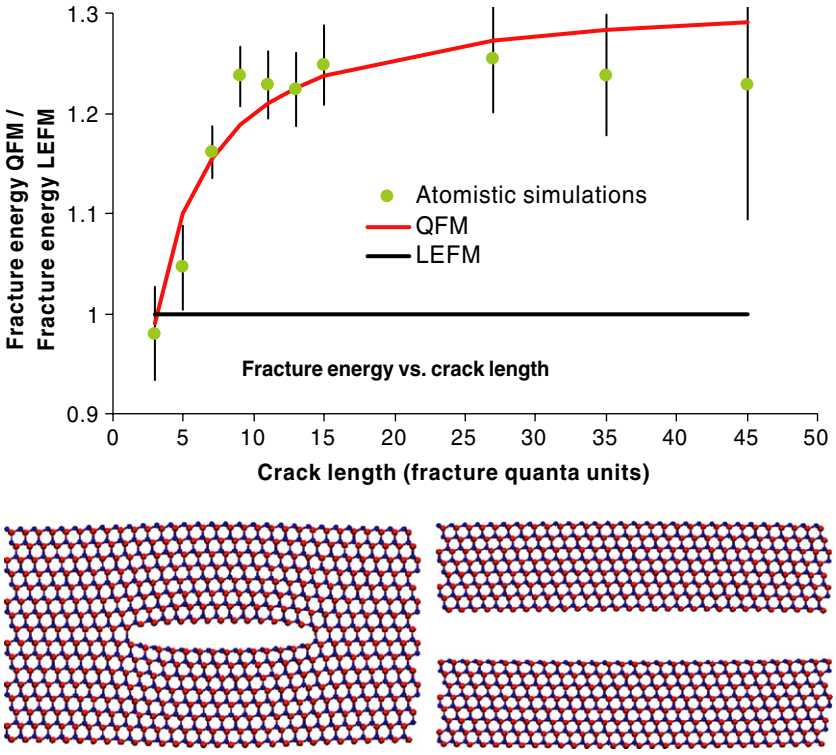

Fig. 4. Comparison between QFM and atomistic simulations. Top: dimensionless crack resistance γ_c as a function of the nanocrack length $2c$. Down: geometry of the crack just before and after failure.

to the Tersoff potential [25]. Such an empirical interatomic potential has already been applied to the study of mechanical properties in β-SiC and it is able to describe the experimentally observed brittle behaviour of cubic β-SiC [26,27]. The same force model has been applied to investigate the strength of β-SiC crystals containing cracks, cylindrical or spherical holes and crack-inclusion interactions.

The typical simulation cell is a cubic thin slab with x, y and z cartesian axes parallel to the [1 1 2], [1 1 0], and [1 1 1] crystallographic directions respectively (Fig. 2). The lowest unrelaxed surface energy of β-SiC is that of the (1 1 1) shuffle plane, having the lowest density of dangling bonds. As a consequence, (1 1 1)-plane cracks are

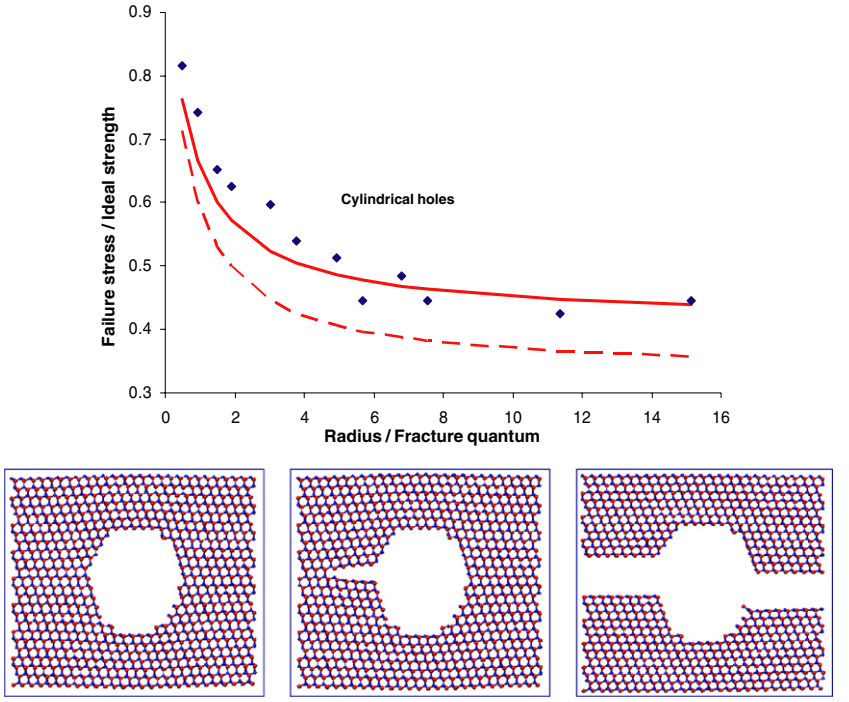

Fig. 5. Comparison between QFM with the elastic–plastic correction (continuous line) and atomistic simulations (dots). The dashed curve ignores the elastic–plastic correction. Top: dimensionless strength as a function of the radius of the cylindrical void. Down: geometry of the cylindrical void just before, during and after failure.

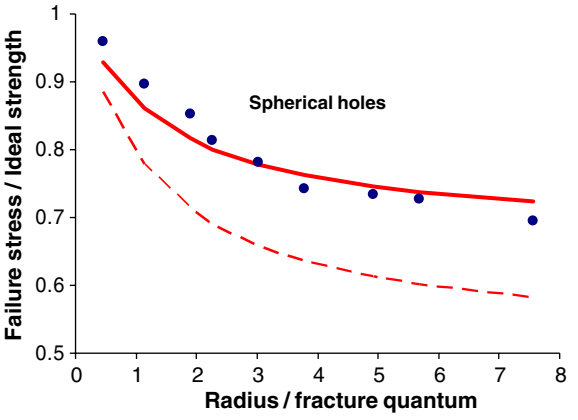

Fig. 6. Comparison between QFM, with the elastic–plastic correction (continuous line) and atomistic simulations (dots). The dashed curve ignores the elastic–plastic correction. Dimensionless strength as a function of the radius of the spherical (inner, thus difficult to be visualize) void.

the most likely to form in experimental conditions, and we have therefore focused our theoretical analysis on such a crack arrangement. Based on the Griffith's formula the critical load increases with decreasing nanocrack length. For the Griffith's theory to be valid, the limits of applicability of linear elasticity must be respected. Such a requirement implicitly defines the minimum length at which a finite-size nanocrack can still be considered a "Griffith's crack". For this reason, and also to prevent finite-size artefacts in the simulation, we varied the actual size of the simulation cell so as to get in any case a ratio $L/c > 10$, where L is the cell dimension along the crack axis.

The external load was applied according to the constant traction method [28]. To this end, the three-dimensional periodic simulation box is initially deformed along the z direction according to a given strain value $\varepsilon = \varepsilon_{[1\,1\,1]}\delta_{zz}$, while keeping $\varepsilon_{xx} = 0$ and $\varepsilon_{yy} = 0$ (plane-strain condition); this corresponds to opening Mode I. Periodicity is then removed along z and surface tractions are calculated in order to preserve the state of deformation. At this stage a defect of given size and shape is introduced by mathematically cutting opportune interatomic bonds. The atomistic stress is obtained either from the value of the average surface traction which preserves the applied strain or, equivalently, from the asymptotic value of the atomic-level virial stress equation [28]. Consistently with the expected brittle behaviour, we have found that at loads above the critical stress σ_c the nanocrack extends in a perfectly brittle way, by preserving atomically smooth (1 1 1) cleavage surfaces, with the exception of interface (matrix/inclusion) cracks.

A series of atomistic simulations was performed with nanocracks of length $c_0 < c < 25c_0$, where $c_0 = 2.644$ Å is the interbond distance along x-direction (Figs. 1 and 2a). To quantify the discrepancy between

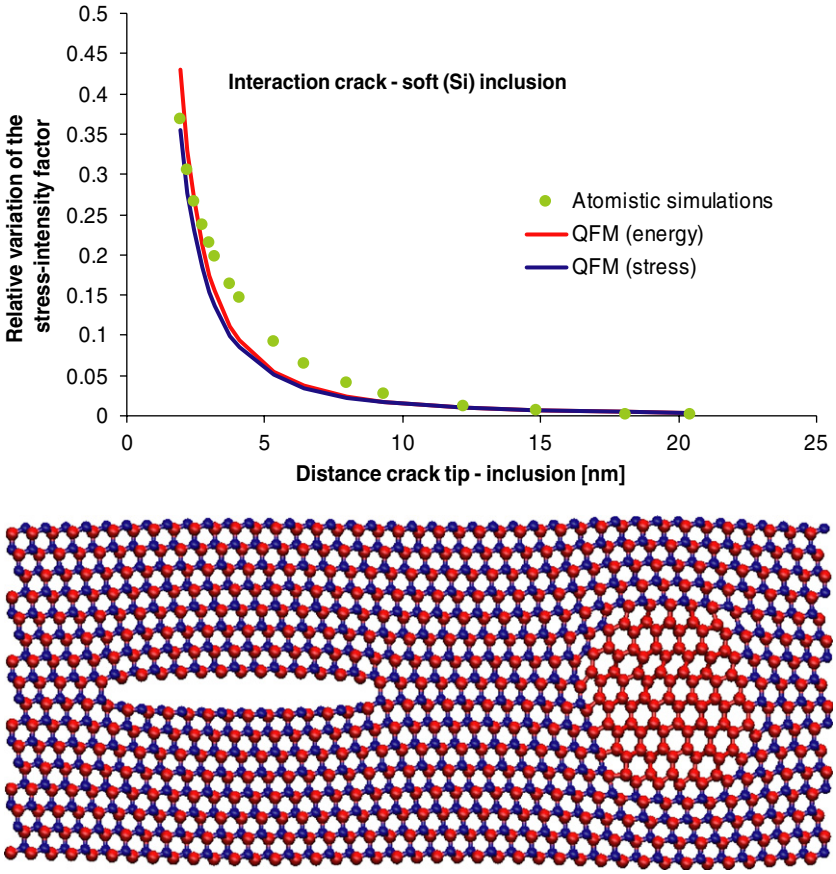

Fig. 7. Comparison between QFM (and Novozhilov's approximation, denoted by QFM-stress) and atomistic simulations. Top: variation of the stress-intensity factor due to the presence of a silicon (soft, red) inclusion as a function of the crack-inclusion distance. Down: geometry of the crack-inclusion interaction. (For interpretation of the references in colour in this figure legend, the reader is referred to the web version of this article.)

the atomistic estimation for σ_c and the critical value of stress predicted by the original Griffith's theory, we have focused our attention on γ_c. In the original form of Griffith's theory γ_c does not depend on the crack length and is therefore a constant: for the previous function an horizontal alignment of the data is expected if Griffith's theory prediction is correct, whereas QFM predicts the law reported in Eq. (1). The results of the present investigation on the physical meaning of the intrinsic crack resistance in the Griffith's theory of brittle fracture are reported in Fig. 4 and compared with the QFM predictions. The atomistic data increase monotonically until reaching an asymptotic limit for long cracks. Such a limit gives a departure of about 25% from the classic Griffith's theory. It is, however, possible to reconcile the above two sets of results by means of QFM which, as previously discussed, takes into account the discrete crack propagation. Referring to Eq. (1) with $c_0 = 2.644$ Å, the best fit of atomistic data is obtained for a radius at tip of $r \approx 0.6c_0$, which is a realistic value, as shown in Fig. 4. The curve predicted by this theory is in good agreement with the atomistic data within the error bars. Note that here we have simply imposed c_0 to be identical to the interatomic distance; furthermore, we have neglected the deviation from the linear elastic constitutive law of the crystal, as a consequence of the moderate strengths of the cracked slabs.

For the cylindrical holes, we have varied the radius in the range 1.3 Å $< R <$ 40 Å, the smallest radius corresponds to the removal of a single row of silicon or carbon atoms. On the other hand, the radius of the spherical holes was 1.3 Å $< R <$ 20 Å, the smallest value corresponding to a single atom vacancy. The atomistically computed hole size-effects can be compared with the QFM prediction of Eqs. (2) and (3), in which $\upsilon \approx 0$, since for β-SiC $\upsilon = 0.05$, see Figs. 5 and 6 respectively. For them, due to the higher failure strains, the elastic–plastic correction proposed in Section 3 is adopted. Still maintaining c_0 equal to the interatomic distance for both

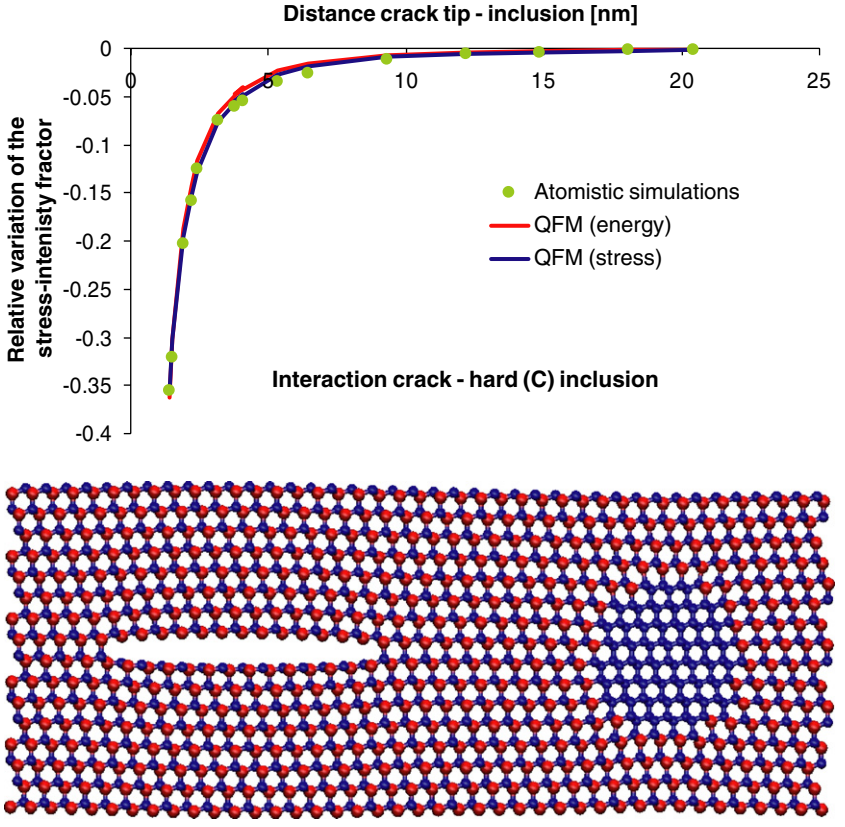

Fig. 8. Comparison between QFM (and Novozhilov's approximation, denoted by QFM-stress) and atomistic simulations. Top: variation of the stress-intensity factor due to the presence of a carbon (hard, blue) inclusion as a function of the crack-inclusion distance. Down: geometry of the crack-inclusion interaction. (For interpretation of the references in colour in this figure legend, the reader is referred to the web version of this article.)

cylindrical or spherical holes, we find the reported best-fits (Figs. 5 and 6) for $\kappa \approx 0.8$ and $\kappa \approx 0.6$ respectively, comparable with the value of $\kappa \approx 0.8$ directly best fitted from the stress–strain curve of Fig. 3. Clearly an alternative solution would be of assuming $\kappa = 1$ and best fit c_0.

Other simulations have been carried out considering a soft (silicon) or hard (carbon) inclusion collinear with the crack and at a given distance d from its closer tip, Figs. 7 and 8 respectively. The stress-intensity factor is evaluated by best fitting the singular stress field near the crack tip. The interaction between crack and inclusion can be compared with the QFM prediction of Eq. (5), see Figs. 7 and 8.

In all the discussed comparisons QFM and MD are found to be in good agreement.

6. Conclusions

The present study points out that in order to take account of all details at the nanoscale in the crack propagation problem, as naturally done by the MD atomistic simulations – which from this point of view can be considered as an ab initio mechanical theory – it is indeed necessary to introduce within the continuum theory the concept of discrete lattice. Such a concept actually defines the discrete space (i.e., the proper lattice) onto which the fracture phenomenon takes place. By ignoring this discrete nature of the medium the well-known paradoxes of the continuum theory are found. As shown in this work the modified continuum theory QFM allows for successfully solve the limits of LEFM analytically.

Acknowledgement

We acknowledge financial support by MIUR under project FISR- PROMOMAT.

References

[1] Griffith AA. The phenomena of rupture and flow in solids. Philos Trans Roy Soc London A 1920;221:163–98.
[2] Lawn BR. Fracture of brittle solids. Cambridge: Cambridge University Press; 1975.
[3] Broberg KB. Cracks and fracture. San Diego: Academic Press; 1999.
[4] Gillis PP. Surface-energy determinations by cleavage. J Appl Phys 1965;36:1374–6.
[5] Rice JR. Dislocation nucleation from a crack tip: an analysis based on the Peierls concept. J Mech Phys Solids 1989;40:239–71.
[6] Curtin WA. On lattice trapping of cracks. J Mater Res 1990;5:1549–60.
[7] Bilby BA, Cottrell AH, Swinden KH. The spread of plastic yield from a notch. Proc Roy Soc London A 1963;272:304–14.
[8] Carpinteri A. Notch sensitivity in fracture testing of aggregative materials. Engng Fract Mech 1982;16:467–81.
[9] Pugno N. A quantized Griffith's criterion. Workshop of the Italian group of fracture on "fracture nanomechanics". 25–26 September 2002, Vigevano, Italy.
[10] Pugno N, Ruoff R. Quantized fracture mechanics. Philos Mag 2004;84:2829–45.
[11] Pugno N. Dynamic quantized fracture mechanics. Int J Fract 2006;140:159–68.
[12] Pugno N. New quantized failure criteria: application to nanotubes and nanowires. Int J Fract 2006;141:311–28.
[13] Taylor D, Cornetti P, Pugno N. The fracture mechanics of finite crack extensions. Engng Fract Mech 2005;72:1021–8.
[14] Pugno N, Ciavarella M, Cornetti P, Carpinteri A. A unified law for fatigue crack growth. J Mech Phys Solids 2006;54:1333–49.
[15] Pugno N, Cornetti P, Carpinteri A. New unified laws in fatigue: from the Wöhler's to the Paris' regime. Engng Fract Mech 2007;74:595–601.
[16] Mattoni A, Colombo L, Cleri F. Atomic scale origin of crack resistance in brittle fracture. Phys Rev Lett 2005;95. 115501-1–4.
[17] Ippolito M, Mattoni A, Colombo L, Pugno N. The role of lattice discreteness on brittle fracture: how to reconcile atomistic simulations to continuum mechanics. Phys Rev B 2006;73. 104111-1–6.
[18] Ippolito M, Mattoni A, Pugno N, Colombo L, submitted for publication.
[19] Novozhilov VV. On a necessary and sufficient criterion for brittle strength. Prik Mat Mek 1969;33:212–22.
[20] Rice JR, Rosengren GF. Plane strain deformation near a crack tip in a power-law hardening material. J Mech Phys Solids 1968;16:1–12.
[21] Carpinteri A, Pugno N. Fracture instability and limit strength condition in structures with re-entrant corners. Engng Fract Mech 2005;72:1254–67.
[22] Carpinteri A. Scaling laws and renormalization groups for strength and toughness of disordered materials. Int J Solids Struct 1994;31:291–302.
[23] Carpinteri A, Chiaia B. Crack-resistance behavior as a consequence of self-similar fracture topologies. Int J Fract 1996;76:327–40.
[24] Ippolito M, Mattoni A, Colombo L, Cleri F. Fracture toughness of nanostructured silicon carbide. Appl Phys Lett 2005;87. 141912-1–3.

[25] Tersoff J. Modeling solid-state chemistry: interatomic potentials for multicomponent systems. Phys Rev B 1989;39:5566–8.
[26] Tang M, Yip S. Atomistic simulation of thermomechanical properties of β-SiC. Phys Rev B 1995;52:15150–9.
[27] Mattoni A, Colombo L, Cleri F. Atomistic study of the interaction between a microcrack and a hard inclusion in β-SiC. Phys Rev B 2004;70. 094108-1–10.
[28] Cleri F. Representation of mechanical loads in molecular dynamics simulations. Phys Rev B 2002;65. 0141071-1–6.